

See discussions, stats, and author profiles for this publication at: <https://www.researchgate.net/publication/373986055>

Investigation of Groundwater Potential Using Geological, Hydrogeological and Geophysical Methods in Federal University of Technology, Minna, Bosso Campus, North Central, Nigeria

Article in *HydroResearch* · September 2023

DOI: 10.1016/j.hydres.2023.09.002

CITATION

1

READS

153

5 authors, including:



Jude Steven Ejepu

Federal University of Technology Minna

40 PUBLICATIONS 144 CITATIONS

SEE PROFILE



Suleiman Abdullahi

Federal University of Technology Minna

7 PUBLICATIONS 27 CITATIONS

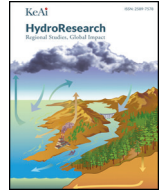
SEE PROFILE



Okechukwu Ebuka Agbasi

115 PUBLICATIONS 847 CITATIONS

SEE PROFILE



Investigation of Groundwater Potential Using Geological, Hydrogeological and Geophysical Methods in Federal University of Technology, Minna, Bosso Campus, North Central, Nigeria

Mufutau Owolabi Jimoh ^a, Glory Tolulope Opawale ^a, Jude Steven Ejepu ^a, Suleiman Abdullahi ^a, Okechukwu Ebuka Agbasi ^{b,*}

^a School of Physical Sciences, Department of Geology, Federal University of Technology Minna, Nigeria

^b Geophysical Unit, Okan Geoservices Nigeria Limited, Nigeria

ARTICLE INFO

Article history:

Received 16 June 2023

Received in revised form 1 September 2023

Accepted 9 September 2023

Available online 16 September 2023

Keywords:

Groundwater capacity
 Geological mapping
 Hydrogeological studies
 Geophysical investigations
 Groundwater potential

ABSTRACT

Groundwater exploration and extraction in challenging hard rock formations with inherent heterogeneity is addressed comprehensively in this study through geological, hydrogeological, and geophysical investigations. Hydrogeological studies assess existing borehole recharge rates and provide an overarching groundwater potential assessment. A 1D Vertical Electrical Sounding (VES) survey, employing the Schlumberger method, acquires sounding data analyzed with WINRESIST software to extract groundwater controlling parameters, revealing distinct geoelectric layers and illuminating groundwater and aquifer system structural control. Geological mapping, employing detailed topographical data, revealed the prevalence of granitic rocks exhibiting quartz vein and joint intrusions, primarily oriented in the NE-SW direction. These geoelectric layers encompassed the topsoil, weathered/fractured granite, and fresh granite, each characterized by apparent resistivity values ranging from 14 Ωm to 572 Ωm, 10.0 Ωm to 408 Ωm, and 1468 Ωm to 19,031 Ωm, accompanied by varying thicknesses. Further insights were gained from isopach and resistivity maps at depths of 10 m and 30 m, identifying areas with low apparent resistivity values and substantial overburden. These findings pinpointed zones with potentially high groundwater potential, particularly in the northeastern and southeastern regions. Additionally, the results from the weathered layer analysis aligned with the isopach and resistivity outcomes. Hydraulic conductivity measurements, falling within the range of 7.00×10^{-5} m/s to 4.31×10^{-4} m/s, confirmed the subsurface materials' capacity to transmit water. Moisture content ranged from 12% to 20%, while infiltration rates varied from 2.675×10^{-4} L/s to 1.259×10^{-5} L/s. Yield test results from three borehole locations yielded production rates ranging from 56.52 m³/day to 364.26 m³/day, although other boreholes returned indeterminate results. Based on the groundwater potential classification, 25% of the area demonstrated high potential, 45% moderate potential, and 30% low potential. Accordingly, the recommendation is to prioritize well or borehole drilling in high-potential areas to ensure optimal water supply management.

© 2023 The Authors. Publishing services by Elsevier B.V. on behalf of KeAi Communications Co. Ltd. This is an open access article under the CC BY-NC-ND license (<http://creativecommons.org/licenses/by-nc-nd/4.0/>).

Introduction

Water, comprising approximately 80% of animal cells, plays a vital role in the proper functioning of the human body (Agbasi et al., 2019). The significance of water as a life-sustaining resource cannot be overstated, as it is crucial for human survival and overall health. Groundwater, with its distinct physical and chemical characteristics, differs from surface water and exhibits greater stability (Agbasi et al.,

2019; Ejepu, 2020). Exploring natural resources like groundwater is of utmost importance and brings numerous benefits to humanity. Two key characteristics of aquifers are their ability to store water (porosity) and facilitate water flow (permeability). There are significant variations among aquifers due to different geological environments, their capacity to store and transmit water, and their influence on well yields (Anomohanran, 2015; Ifeanyichukwu et al., 2021; Akaolisa et al., 2022a). Groundwater recharge occurs through various sources including meteoric recharge and paleo-atmospheric precipitation. Other sources may come from surface water bodies like rivers, lakes, and wetlands, as well as human activities like irrigation. (Ejepu et al., 2017; Sophocleous, 2000; Trabelsi et al., 2020). The occurrence of groundwater is highly influenced by the regional geological setting, which also

* Corresponding author.

E-mail addresses: mo.jimoh@futminna.edu.ng (M.O. Jimoh),
 ejepu.jude@futminna.edu.ng (J.S. Ejepu), absuleiman@futminna.edu.ng (S. Abdullahi),
 agbasi.okechukwu@gmail.com (O.E. Agbasi).

affects well yields (Sikakwe, 2018; Ajayi et al., 2021). The recharge of aquifers is crucial for maintaining a balance between water removal and replenishment (Sophocleous, 2000).

Consequently, it is necessary to know the hydrogeological environment and precisely classify aquifers in order to effectively distribute and manage groundwater resources (Ejepu et al., 2022). Groundwater mapping acts as a vital instrument in water development activities, delivering insights into the distribution of groundwater resources and possible options for water delivery (Oyedele, 2019; Epuh et al., 2020). By adopting this technique, cost efficiency is fostered, and the rapid expansion of water access for the Nigerian people is facilitated.

Water is essential within the university for various purposes such as drinking, food preparation, hygiene, irrigation, animal care, and commercial and industrial activities (Ejepu and Olasehinde, 2014). Access to water is a fundamental right for all staff and students, but unfortunately, a significant number of people in the study area still lack adequate access. Previous efforts have been made to improve water supply within the university, but there is still a gap that needs to be addressed.

The Bosso campus of the Federal University of Technology, Minna, depends partly on water supplied by the Bosso dam and mostly on groundwater drawn from motorized and hand-pump boreholes. However, during the dry season, the campus experiences water scarcity and associated issues due to increasing demand and the restricted storage and transmission capacities of the underlying basement geological structure in the area. It is crucial to know the storage and transmission capacity of the subsurface geology within the campus to find more productive wells and properly manage the water supply in a sustainable manner.

The Vertical Electrical Sounding (VES) method is extensively employed for electrical resistivity surveys. This technique evaluates disparities in vertical electrical resistivity by passing current through inserted electrodes and measuring potential differences using other electrodes (Ejepu and Olasehinde, 2014). A direct current is used from a dry cell, forming the foundation for geoelectric data analysis. The obtained resistivity, known as “apparent resistivity,” is a result of measuring induced current and potential difference. While this measurement assumes uniform ground, real-world conditions unveil variable resistivity due to geological distinctions. To address this, a graph correlating apparent resistivity with current electrode spacing is used to identify vertical resistivity changes. This analysis yields accurate resistivity readings, layer depths, and aids in detecting groundwater presence. Key factors influencing groundwater estimation encompass aquifer thickness and the degree of pore space interconnection within the material [4], which subsequently affects an aquifer's groundwater storage and transmission capabilities (Ifeanyichukwu et al., 2021).

For the sustainable utilization of groundwater resources, it is essential to incorporate aquifer parameters acquired through pumping tests and other pertinent hydrogeological measurements like moisture content and particle size distribution analysis of the overlying formation. Pumping tests involve the controlled extraction of water from a test well, followed by water level measurement during a defined period (Singh, 2001). The difference between the measured and static water levels provides drawdown values essential for estimating transmissivity and hydraulic conductivity. Particle Size Distribution (PSD) is a significant soil property directly determining soil texture classification and substantially impacting aquifer attributes (Anomohanran, 2013). Moreover, the integration of in-situ infiltration data and other hydrogeological information is increasingly vital for comprehending recharge dynamics and identifying suitable recharge sites.

Hence, the objective of this study was to ascertain the groundwater potential and aquifer characteristics of the University area, serving as a guide to delivering high-quality, sustainable water to the community. Hydrogeophysical and hydrogeological methods were employed to determine groundwater potential and assess groundwater aquifer attributes.

Study Area Description

The research region, illustrated in Fig. 1, is positioned within the geographical coordinates of longitudes 6°31'20.01"E to 6°31'45.05"E, relative to the Greenwich meridian, and latitudes 9°38'56.7"N to 9°39'30.02"N, related to the equator. It encompasses an estimated size of around 294.7 km². The research location is part of Minna Sheet 164SW, situated in the North Central area of Nigeria. More specifically, it is located in Minna, which serves as the capital city of Niger State.

The study area can be accessed via Lambata and Bida expressways in the southwestern part, as well as Zungeru in the northwestern part. It features a relatively flat landscape with gentle hills and is intersected by the Chachanga River and its tributaries. The surveyed location presents predominantly level terrain with gentle hills and is drained by the Chachanga River, which is accompanied by tributaries going through the urban areas of Maikunkele and Maitumbi in Minna (Ejepu and Olasehinde, 2014). Along the river channels, the flora takes on a more forest-like aspect. The bulk of tributaries in the study area drain into a well-constructed concrete canal that stretches from the north-eastern edge of the school to the southern portion of Minna city. The study area benefits from a durable and properly engineered concrete drainage system.

The research area observes two different seasons: the dry season and the rainy season (Ajibade, 1982). Temperature fluctuates from roughly 21 °C during the peak of the rainy season (December and January) to 35 °C during the height of the dry season (March and June) (Federal Meteorological Agency Minna, 2011). The vegetation in the studied area sits within the center part of the savannah and exhibits traits that lie between the wooded zone of Southern Nigeria and the numerous forms of Guinea Savannah found in Northern Nigeria. The area is characterized by thick grasses with scattered trees. During the dry season, tree distribution is poor, whereas in the rainy season, they are more equally dispersed.

The examined region is located in the northern-central section of the Nigerian Basement Complex, typified by three separate lithofacies: earlier granites, a low-grade schist belt, and the migmatite gneiss complex (Olawaju et al., 1996; Olasehinde, 1999). Within the study region, a concrete wall canal stretches through the Minna settlement and the whole Bosso Campus. The aquifer in the area is replenished by precipitation, resulting in increased discharge from boreholes that tap into regolith aquifers during the rainy season compared to the dry season (Amadi et al., 2013).

The hydrogeology of the area can be described in the context of a typical Basement Complex region comprising primarily of two prominent aquifer units: the weathered and fractured Basement aquifers (Ejepu and Olasehinde, 2014; Ejepu et al., 2017). The Basement Complex rocks are most times overlain by a sequence of loosely consolidated superficial deposits and Basement regolith, which arises from the prolonged weathering of the parent rock. Rocks containing abundant unstable ferromagnesian minerals have a propensity to erode into clay, potentially leading to the formation of micaceous impermeable rock structures that exhibit poor groundwater discharge. Conversely, rocks rich in stable minerals like quartz tend to disintegrate, forming porous and permeable water-bearing mediums with gravelly or sandy attributes (Offodile, 2002).

The weathered layer aquifer may manifest individually or in conjunction with the fractured aquifer. Aquifer combinations in the Basement Complex area have been delineated by Olorunfemi and Fasuyi (1993) to encompass the weathered layer aquifer, weathered/fractured (unconfined) aquifer, weathered/fractured (confined) aquifer, weathered/fractured (unconfined)/fractured (confined) aquifer, and the fractured confined aquifer.

The hydrogeological characteristics of rocks are chiefly determined by porosity and permeability, with these attributes contingent upon the texture and mineral composition of the rocks. In the case of fresh, non-fractured crystalline rocks, porosity typically remains below 3%,

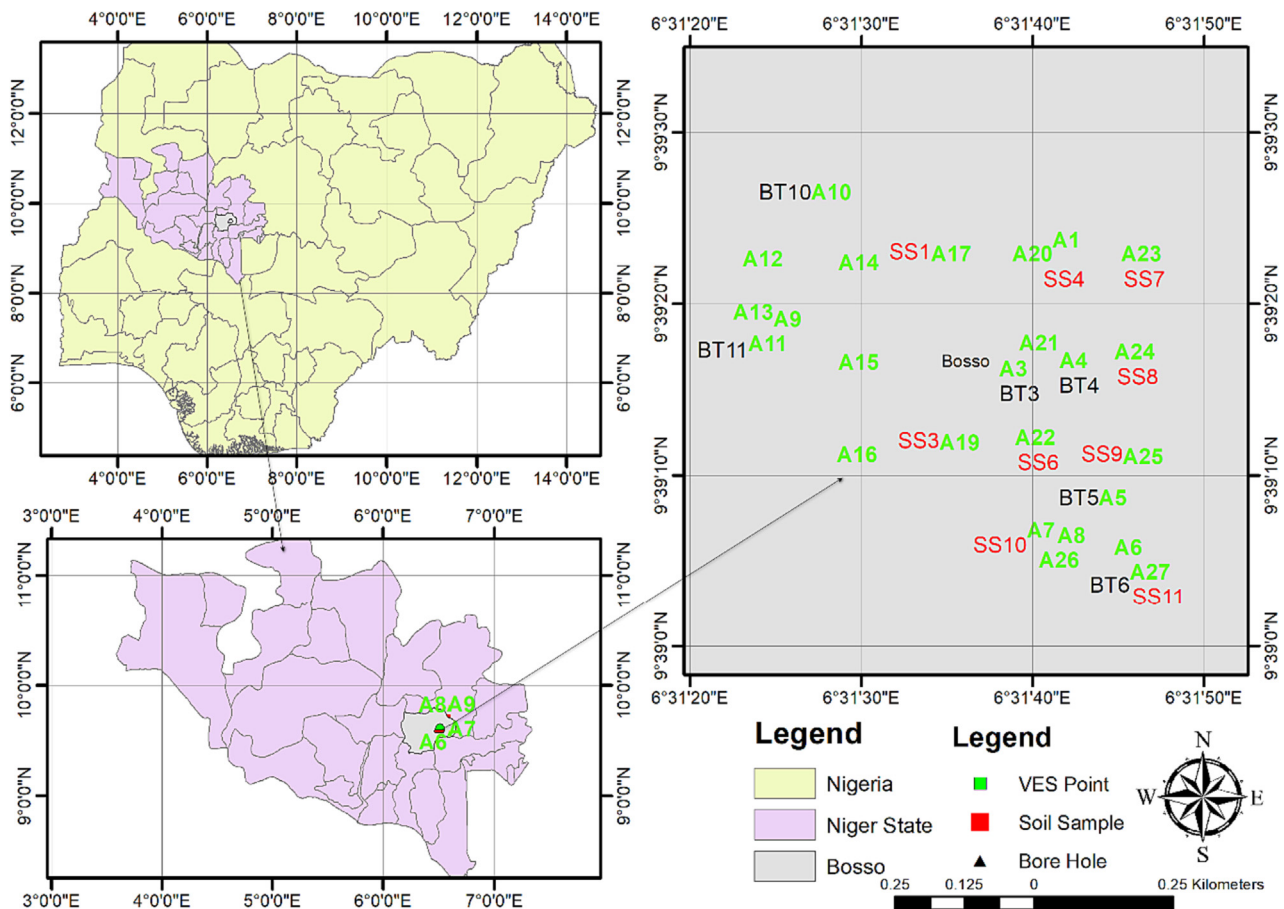


Fig. 1. Map of the study area with VES, Bore Hole and Soil Sample points.

and permeability is nearly negligible. Nevertheless, weathering and fracturing processes lead to a notable increase in both porosity and permeability (Offodile, 2002). It's worth noting that aquifers within the Basement rocks are notably constrained in both their horizontal and vertical extent.

Methodology

Materials

This study focused on analyzing two main natural resources: soil samples and water. Soil samples were collected in the field during the rainy season, and each sample weighed approximately 2 kg. Six different locations were selected, and soil samples were taken at a maximum depth of 1.5 m for sieve analysis. Soil moisture content experiments were conducted at a depth of 0 m. Infiltration field experiments were performed using 446.16 cm³ of water to determine the infiltration rate of the geological material. The time taken for the water to fully penetrate the ground was recorded.

The research involved collecting primary data through fieldwork and laboratory testing, which included determining resistivities of geological layers, creating maps, analyzing sieve data for hydraulic conductivity, and measuring soil moisture content. Additionally, secondary data, including rainfall records and borehole yield tests, were obtained from external sources for further analysis.

Methods

Rainfall

In the study area, rainfall is the major supply of water, and a seasonal stream runs through the region during the rainy season. To analyze the

water availability, rainfall data was gathered and utilized to compute the average annual rainfall (AAR) by evaluating the rainfall over a three-year period. This supplied crucial information on the general wetness of the area and helped identify potential rainfall deficiencies. The index of wetness was established using a particular formula:

Index of wetness

$$= \frac{\text{rainfall in a given year at a specific location (mm)}}{\text{average annual rainfall of that location (mm)}} \quad (1)$$

The resulting index of wetness was characterized as wet (good), dry (bad/difficult), or normal (average) depending on whether the rainfall was higher than, less than, or equal to the average annual rainfall, respectively.

Sieve Analysis and Soil Moisture Content

Hydrogeological research in the study region involved several ways of analyzing groundwater and surface water, concentrating on the specific soil features. Six trial pits were methodically and randomly selected around the research region to gather soil samples. At each pit, samples were collected at four different depths (0 m, 0.5 m, 1 m, and 1.5 m) for sieve analysis. In two places, water crept into the trial pits at depths of 0.5 m and 1 m owing to soil saturation. A tiny bowl was used to drain the water and aid digging. The collected samples were tagged and delivered to the laboratory for sieving examination. Additionally, soil moisture content samples were obtained at ground surface level in six sites.

Infiltration Rate

Simultaneously with the collection of soil moisture content and sieve analysis samples, an on-site infiltration rate experiment was undertaken. The experiment involves the use of several equipment and

supplies, including a shovel, a 2 kg hammer, a timer, a 10-l bucket, lumber or a small block of wood, water, a small bowl, and a cylindrical container.

Borehole Yield Test

Pumping tests entail draining groundwater from a well at a constant pace while monitoring water levels in the pumped well and surrounding observation wells or surface water bodies. This method gives a practical and trustworthy strategy for evaluating well performance, establishing aquifer features, and measuring the impacted region (Balasubramanian, 2017).

To estimate the well performance and understand the recharge from nearby subsurface water sources, a yield test was conducted using the modified Cooper and Jacob method (Anomohanran and Iserhien-Emekeme, 2014; Gomo, 2018). Pumping test data for boreholes were collected from Geoxplore Nigeria Limited, and the pumping test calculations were performed based on the Cooper and Jacob method. This allowed us to determine the aquifer's yield in the study area.

Resistivity Survey

The resistivity survey aimed to assess subsurface resistivity and rock characteristics by measuring the ground surface. It enabled the determination of geological sequences and structures, particularly regarding layer thickness and depth variations (Ajayi et al., 2021). The investigation utilized the GeoSensor, a high-impedance voltmeter known for its precision and accuracy in various geophysical surveys such as environmental, engineering, structural mapping, and hydrogeology (Ahamefula et al., 2012; Ayolabi et al., 2004).

For the vertical electrical sounding (VES) method, the Schlumberger arrangement was employed with a maximum AB/2 of 100 m. The electrode spacing increased outwardly from the center to capture horizontal layering information of subsurface strata. To enhance vertical resistivity resolution, MN potential electrodes remained fixed at predefined intervals, while AB/2 current electrodes were incrementally positioned outward. Increasing AB/2 corresponded to greater penetration depth, resulting in a rapid decrease in the measured potential difference at MN/2 electrodes (George et al., 2022; Adewumi et al., 2023). Adjusting the MN electrode spacing compensated for near-surface inhomogeneity, ensuring a more reliable response. Overlapping MN measurements were used to interpolate any shifts in the sounding curve (Reinhard, 2006).

Eleven VES stations were aligned with existing boreholes, while an additional 16 stations were strategically located using a grid map. In total, there were 27 VES stations across the campus, with red color points indicating the locations of the geophysical survey (vertical electrical sounding). Most VES stations had a maximum current electrode spacing of 100 m, except for a few cases where structures or constructed roads in the investigated zone limited the spacing. The map displayed 11 VES stations across existing boreholes as A1 to A11, and the remaining 16 VES stations were denoted as BT1 to BT16 (Fig. 1).

Laboratory Analysis

The purpose of conducting index geotechnical tests, such as sieve analysis (Grain Size Distribution) and moisture content measurement, was to categorize the soil samples based on their physical qualities. The analysis follows the American Standard Testing Method (ASTM) criteria (Ilan and Charles, 2019). Soil Moisture Content Soil moisture content represents the total amount of moisture present in a material, usually expressed as a percentage of the material's actual bulk. There are different approaches to measure moisture content, including internationally accepted moisture meters or oven-dry analyses.

Soil moisture content research is essential to understand the water-holding capacity of the soil at the sampled location. Soil samples were taken at six separate places from a depth of 0 m, and the moisture content samples were dried in an oven for 24 h. The examination entailed the use of several equipment, including an electric

weighing scale, an oven with an oven thermometer, a dry container, and a sample tray.

The concept of soil moisture content centers on the understanding that, in natural settings, moisture within the soil primarily originates from rainfall or irrigation. When the soil becomes saturated with water, it occupies the spaces that were previously filled with air. As the water content increases, it eventually saturates all the available pores in the soil. Any surplus water beyond what the soil can hold will then move downward through the soil layers until the rainfall or irrigation stops. (Robinson et al., 2008). In laboratory examination, the weight of moist soil encompasses both the weight of dry soil particles and the weight of water. When water is added to the soil, the weight of the wet soil increases while the weight of the dry soil particles remains constant. In laboratory settings, soil moisture content is often stated based on the dry weight to achieve uniform results (Ilan and Charles, 2019).

Sieve Analysis (Grain Size Distribution)

The soil samples acquired from six separate locations at depths of 0 m, 0.5 m, 1 m, and 1.5 m were permitted to dry naturally in the air for a period of 5 to 7 days prior to completing the sieve examination. The laboratory technique entailed employing a weighing scale, mortar and pestle, soil pulverizer, set of sieves, toothbrushes (soft and hard bristles), a mechanical sieve shaker, a beaker, and a washing pan.

The sieve analysis process involved obtaining a soil sample from the field and air-drying it. The dried sample was then pulverized and transferred to a pan for weighing. A nest of sieves, including various sizes and a pan, was prepared according to ASTM standards. The sieves were subjected to mechanical shaking to separate the soil particles. After shaking, the retained materials on each sieve were weighed, and the weights were compared with the initial sample weight to analyze the particle size distribution (Akaolisa et al., 2022b).

During the sieve analysis, different computations were carried out. The weight of the dirt kept on each sieve was calculated by subtracting the weight of the empty sieves and the pan from the overall weight. This retained soil weight was then compared to the initial weight of the soil sample before sifting, and if there was a soil loss of around 2%, the experiment was repeated. The proportion of soil kept on each sieve was estimated by dividing the weight of the retained soil on each screen by the original sample weight. To determine the cumulative percentage of finer particles by dry weight, the weight percent passing, reflecting the proportion of particles that went through the sieves, was calculated.

Groundwater Potential map

Geophysics and hydrogeology data from multiple sources were utilized to construct maps for different input parameters. These parameters included isoresistivity, depth to basement, weathered layer resistivity, thickness of the weathered layer, hydraulic conductivity, soil moisture content, and infiltration rate. The data/maps were plotted and layered using ArcGIS software. Each element played a key part in measuring groundwater potential and was rated appropriately. Classes were assigned to the variables based on their hydrogeological qualities, and a groundwater potential map of the area was developed. Percentage numbers were assigned to each class to illustrate their respective effect on groundwater potential.

Results and Discussion

Geological Mapping

The Precambrian Basement Complex dominates the research area in Nigeria, with granite being the most dominant rock type at the Federal University of Technology, Minna's Bosso Campus. Granite is abundant in the northern part of the country and may be found throughout. Field samples range in texture from fine to medium grain, including major minerals such as Biotite, Quartz, and Feldspar. The granite is leucocratic,

which means it has a larger amount of quartz and feldspar, as well as some Biotite. Weathering induced by variables such as rainfall and temperature, as well as human activity and vegetation, has exposed the granite and resulted in the appearance of cracks and joints. Fractures occur when stress surpasses the elastic limit of the rock. These fractures are significant in groundwater systems as they allow water to move through the rock by providing permeability. The condition of the aquifer depends on the rate of fractures, which can vary. In the observed area, the predominant type of fractures is joints. They range in length from 3.5 m to 8.0 m, with widths ranging from 0.01 m to 0.15 m. These fractures align in the NE-SW direction.

The joints observed in the field are referred to as tectonic joints because they result from brittle deformation in rocks. They exhibit various orientations, such as 40°, 310°, 22°, and others. Some joints have been healed by the deposition of quartz or quartzofeldspathic minerals. The principal direction of the joints in the field is predominantly NE-SW, as depicted in Fig. 2's rose diagram. The majority of outcrops in the area exhibit parallel joints, except for those close to the staff school (N9° 39' 24.2", E6° 31' 29.2"), where numerous orthogonal joints intersect each other in different directions.

Quartz veins and quartzofeldspathic veins are mineral deposits that form when new minerals fill pre-existing fractures or fissures within a host rock. They appear as sheet-like bodies of crystallized minerals within the rock. These veins were traditionally believed to have formed through crystal growth on the walls of planar fractures in the rocks. The measured orientations of the veins were 254°, 83°, 64°, 92°, 55°, 32°, 70°, and 232°. The high feldspar content of these rocks, coupled with interactions with water, can lead to chemical weathering, potentially resulting in the formation of clay minerals during weathering.

Exposed fractured granitic rocks and a thin coating of regolith suggest possible drill locations. The principal source of groundwater is fractured basement aquifers. Through fracture distribution and weathering processes, cracked bedrock works as conduits for groundwater transport, influencing hydrogeology.

Rainfall Data

Rainfall data for the study region was received from the Department of Geography at the Federal University of Technology, Minna. This data

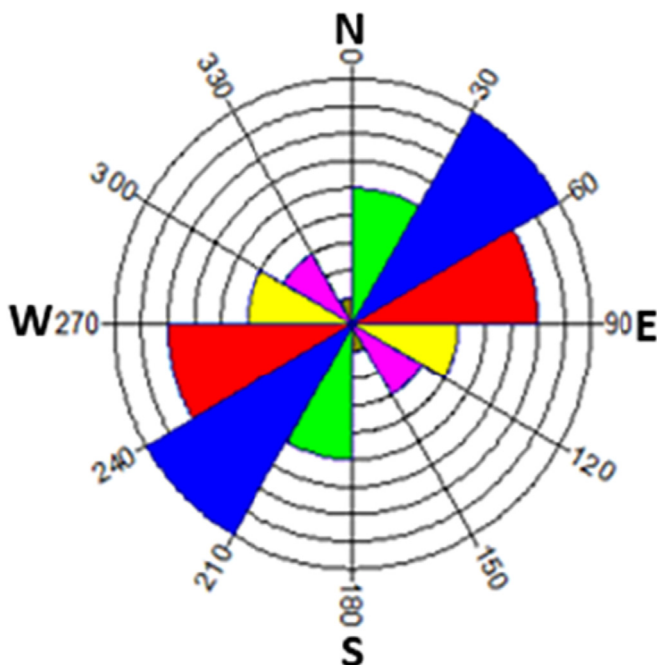


Fig. 2. Rose diagram.

was used to determine the average annual rainfall (AAR) and the index of wetness for categorization purposes. Monthly rainfall data and a matching bar chart were gathered for three consecutive years: 2017, 2018, and 2019. The examination of the monthly data found that rainfall occurred throughout a duration of seven months in the research region, with occasional exceptions in March, except for the year 2017 when it lasted for six months. Among the three years, 2019 received the most rainfall with a maximum of 353.6 mm in March, while the lowest rainfall was 3.5 mm in September. The minimal rainfall regularly happened early in the year, such as in March or April, while the highest rainfall typically fell throughout the mid-year months of July, August, and September. In 2019, the Nigerian Meteorological Agency forecasted variable amounts of rainfall across the nation, ranging from 300 mm in the north to 2700 mm in the south (Nigerian Meteorological Agency, 2019).

Soil Moisture Content

The data relating to soil moisture content are described in Table 1. The computed values of soil moisture content ranged from 17.73 to 21.07, with corresponding moisture percentages varying from 14% to 20%. These data represent the moisture levels present in each soil sample obtained at the time, demonstrating potential differences in moisture content based on prevailing weather circumstances.

The data received from the computation of soil moisture content, combined with the infiltration rate statistics for the region, were applied for a complete analysis to meet the research objectives. Among the different sites, Location 5 displayed the greatest percentage of moisture content, while Location 8 presented the lowest. This shows that Location 8 has increased permeability and porosity compared to Location 5. It is probable that an impermeable layer, presumably made of silt or clay, exists in Location 5, unlike the other places. By combining the results of soil moisture content with the data from the infiltration rate experiment and field observations, it can be determined that Location 5 includes an impermeable layer, whereas Location 8 holds a porous layer.

The findings of the Soil Moisture Content were employed in conjunction with the coordinates of the location to build a soil moisture content map. This map demonstrates the variance in moisture content across the research region at the time of sampling in the field. The map demonstrates that moisture content increases towards the north-western and south-western areas of the research region, whereas the middle and south-eastern parts display lower levels of moisture (Fig. 3).

The computed weight of soil moisture content ranged from 18.07 to 21.07, with corresponding moisture percentages ranging from 12% to 20% at Location 5 and Location 8, respectively. Location 5 had the largest percentage of moisture content, while Location 8 had the lowest.

Infiltration Rate

The recorded values of infiltration range from 1.259×10^{-5} l/s to 2.675×10^{-4} l/s. These values indicate the rate at which water vertically infiltrates the ground surface over a given period of time. (Fig. 4). This information allowed for an assessment of the rate of water movement

Table 1
Soil moisture content parameter for all the locations.

Soil moisture content						
Location No	5	6	8	9	11	12
Weight of Can (g)	23.55	23.40	23.20	22.99	22.83	23.94
Weight of Can + Wet Sample (g)	150.35	208.73	191.67	158.38	170.89	163.85
Weight of Can + Dry Sample (g)	129.28	187.77	173.60	138.38	153.16	143.56
Weight of Dry Sample (g)	105.73	164.37	150.40	115.39	130.33	119.60
Weight of Moisture (g)	21.07	20.96	18.07	20.00	17.73	20.29
Moisture Content (%)	20%	13%	12%	17%	14%	17%

from the surface to the subsurface. The north-western parts of the study area exhibited slower water movement compared to other regions (Fig. 4). These findings contribute to our understanding of surface water movement before it percolates into the subsurface.

The infiltration rate data for Location 6 and Location 8 at different depths is shown in Fig. 4. For Location 8, at a depth of 0 cm, the time and duration of measurement were recorded as 2:33 pm to 6:07 pm. Similarly, at a depth of 3 cm, the measurement was collected from 2:33 pm to 6:07 pm. The time and length of measurement grew as the depth climbed, with the last recorded depth at 21 cm, measured from 3:39 pm to 6:35 pm, with a duration of 23 min.

For Location 6, the measurements followed a similar trend. The length and duration of measurement grew as the depth climbed, with the maximum depth recorded at 21 cm, measured from 6:10 pm to 6:35 pm, with a duration of 6 min. The overall period of the infiltration rate measurement for Location 8 was 1 h and 7 min, whereas for Location 6, it was 28 min. The infiltration rates for Location 8 and Location 6 were reported at 1.110×10^{-5} L/s and 2.656×10^{-5} L/s, respectively.

Grain Size Distribution Characteristics

The analysis of particle size distribution for the soil sample at Location 5 is presented in Fig. 5. Based on the results of the particle size distribution analysis, the soil retained on the ASTM sieve at different depths ranged from 63.7% to 88.0% at 0 m, 53.2% to 84.0% at 0.5 m, 68.6% to 88.3% at 1.0 m, and 31.5% to 88.0% at 1.5 m.

These findings indicate that a significant portion of the soil samples, ranging from 63.7% to 88.0%, 84.0%, 88.3%, and 88.0% at depths of 0 m, 0.5 m, 1 m, and 1.5 m, respectively, consists of grains classified as coarse sand to fine sand. This suggests that the soil is permeable and porous, allowing water to move easily through the sand. Water can flow freely through the open spaces (pores) between the sand grains, enabling it to move towards regions of lower hydraulic head.

Hydraulic Conductivity

The computed hydraulic conductivity varies from 7.00×10^{-5} m/s to 4.31×10^{-4} m/s for position 5 and location 12, respectively. These

values fall within the permissible range for fine to coarse grain sands, as specified by Domenico and Schwartz (1998) and Newman et al. (2021). The hydraulic conductivity map, displayed in Fig. 6, reveals differences in permeability across the research region. The south-eastern regions display better permeability to water compared to the north-western part. This shows a reduction in water flow towards the north. The field experience during soil sample collection for grain size analysis also confirms this conclusion, with the north-western section being tougher and more time-consuming compared to the south-eastern part.

Borehole Yield Test

Data on the hydraulic characteristics of water-bearing rocks was acquired through pumping tests. These tests gave insights into numerous factors including as resistivity, infiltration rate, hydraulic conductivity, and moisture content. Based on the results, locations with low resistivity, high infiltration rate, high hydraulic conductivity, and low moisture content were identified as having the potential for good water output compared to other places. These data, in combination with the aforementioned approaches, can be used to estimate the water yield potential of different places.

The particular parameters for borehole yield, together with their related locations, are provided in the borehole yield chart, as shown in Table 2.

Geophysical Studies

Vertical Electrical Sounding

In this study, the Winresist software was utilized for interpretation, which revealed the presence of three distinct geoelectric layers in all locations: the topsoil, fractured/weathered basement, and fresh basement. The first layer exhibited apparent resistivity values ranging from 14.1Ωm to 571.9Ωm, with a thickness ranging from 0.5 m to 4.6 m. The second layer had apparent resistivity values ranging from 10.0Ωm to 406.9Ωm, with a thickness ranging from 2.0 m to 13.1 m. The third layer displayed apparent resistivity values ranging from 1467.6Ωm to 19,031.2Ωm, with an infinite thickness.

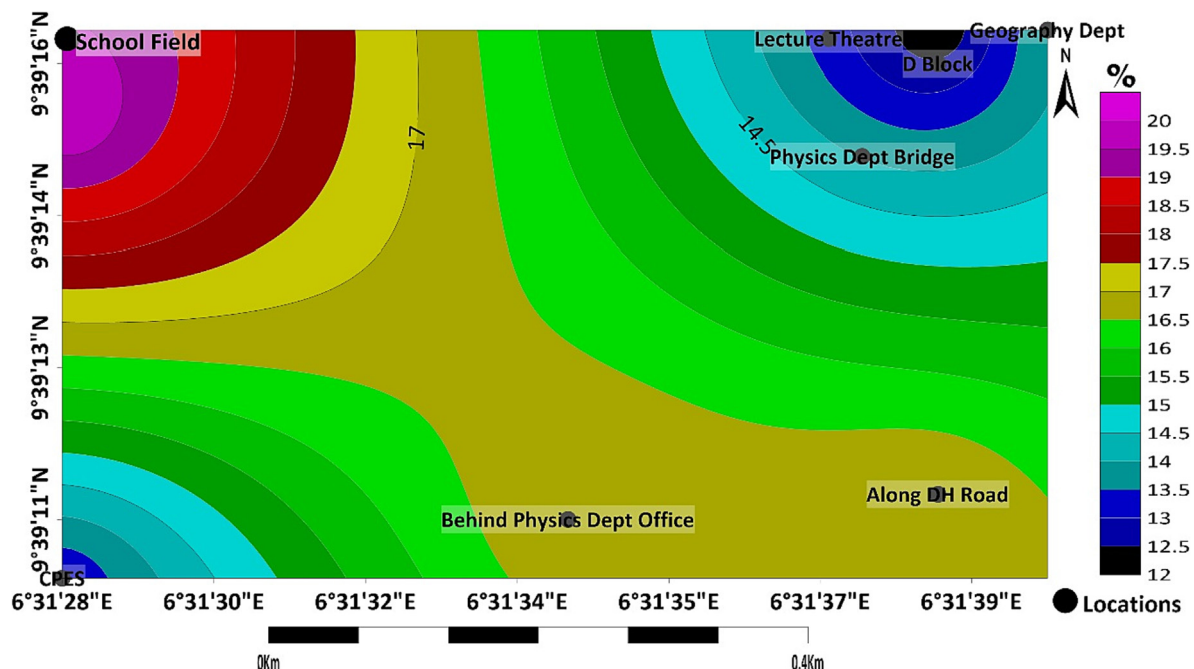


Fig. 3. Soil moisture content map.

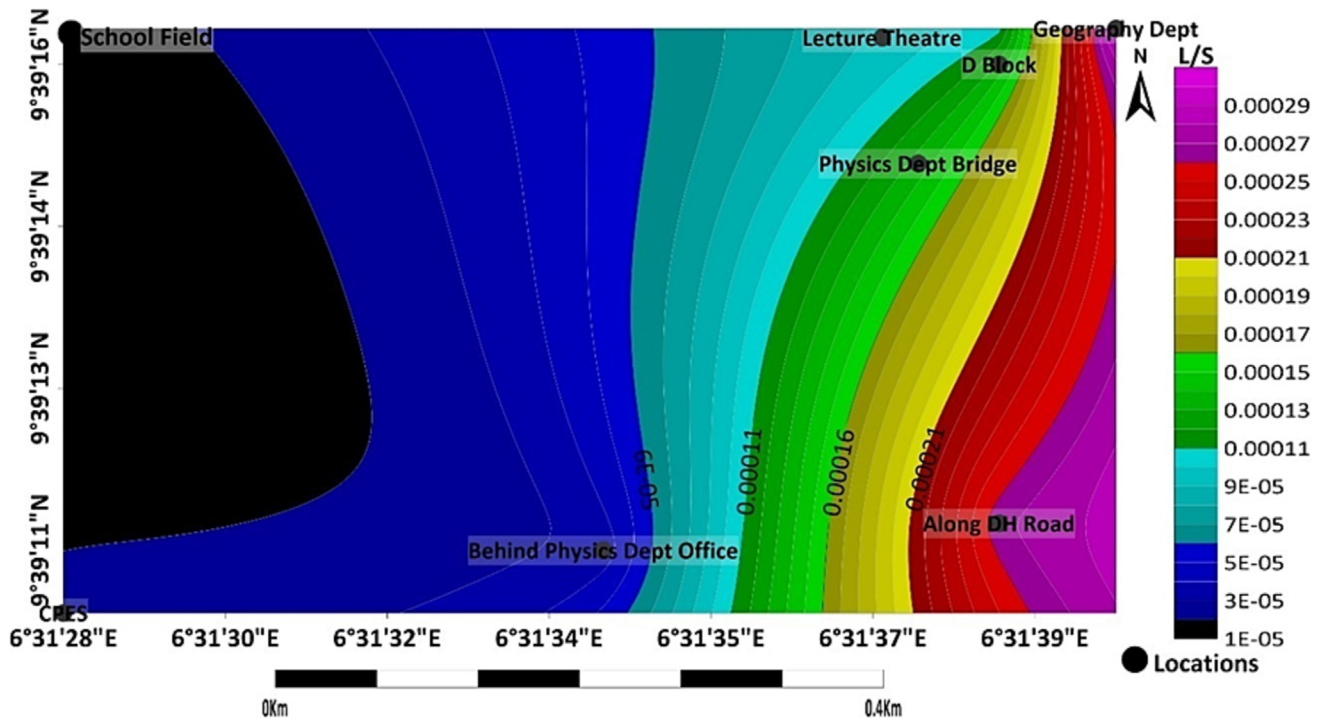


Fig. 4. Infiltration rates for Location 8 and Location 6.

The use of the 1D electrical technique, particularly Vertical Electrical Sounding, has been extensively employed in previous studies to differentiate aquifers in various geological terrains and to map fractured areas within the basement (Ahamfula et al., 2012; Ayolabi et al., 2004). The observed resistivity curve types were A and H-type curves.

Iso-resistivity Maps

The maps given in Figs. 7, 8, and 9 exhibit lines linking places with identical electrical apparent resistivity, known as iso-resistivity. In this study, the iso-resistivity values at depths of 10 m, 30 m, and 80 m were evaluated.

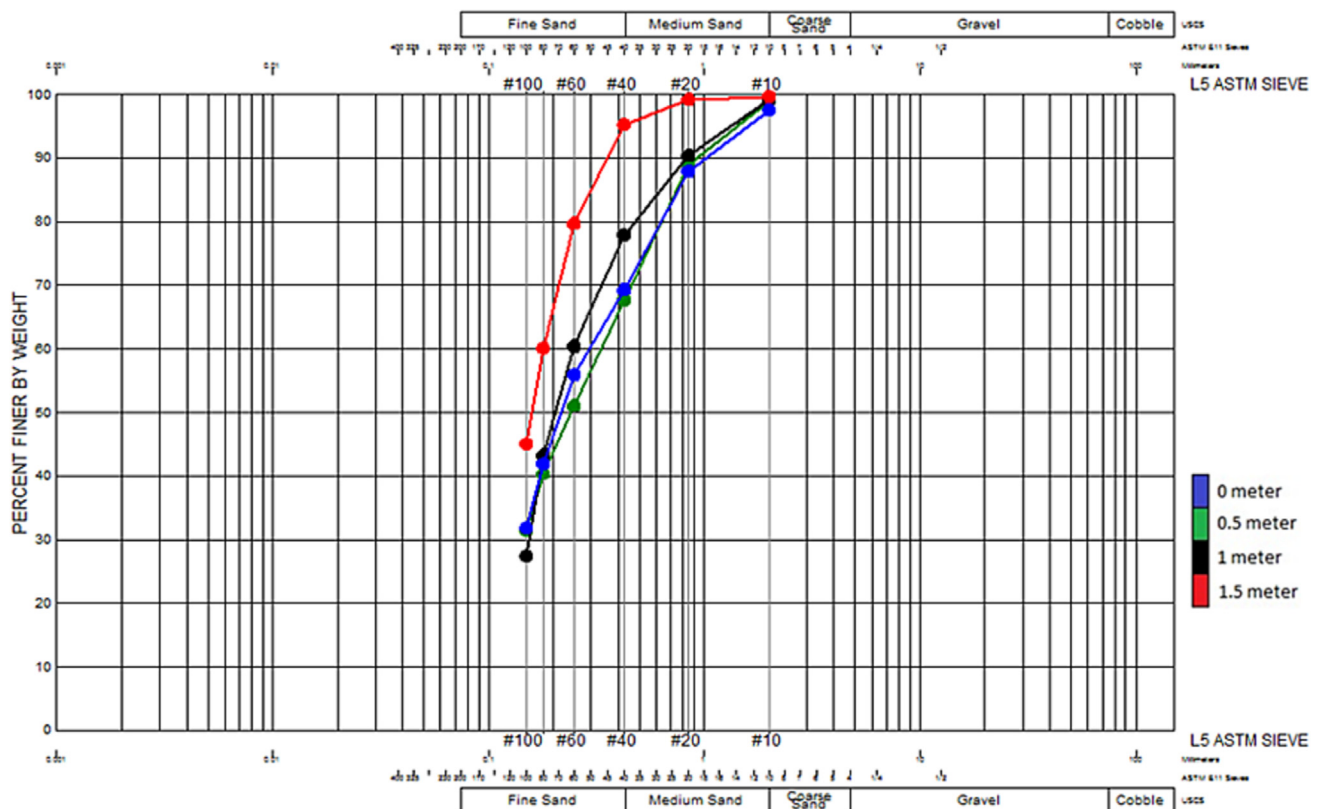


Fig. 5. Grading curve for Location 5.

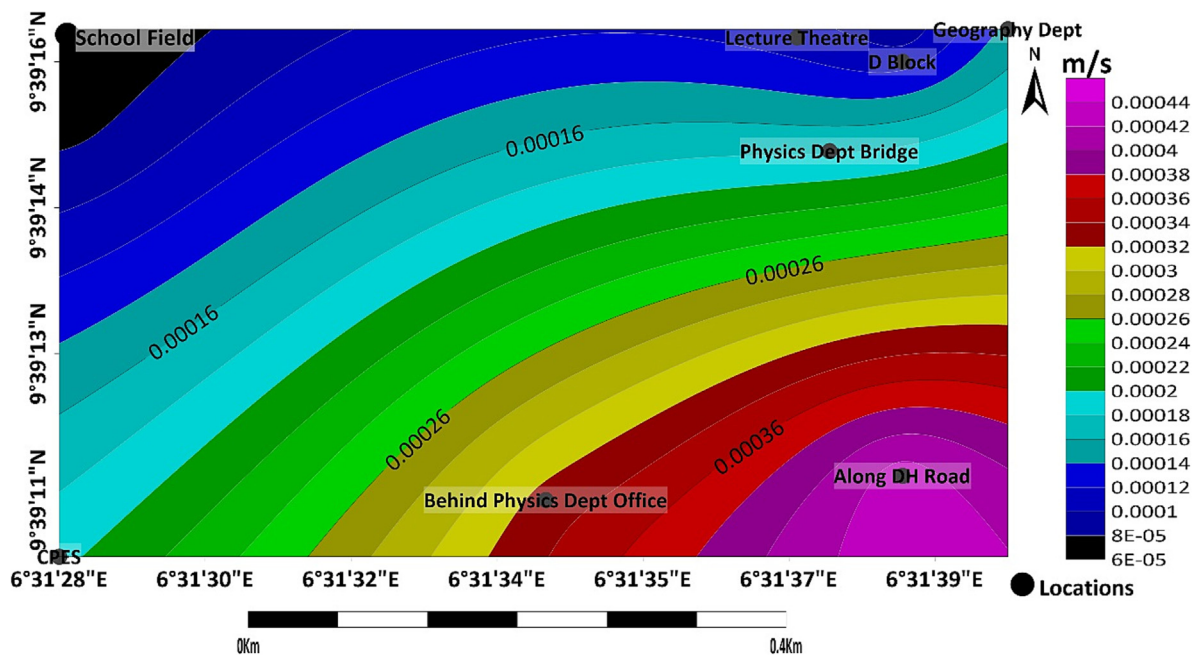


Fig. 6. Hydraulic conductivity map.

Iso-resistivity at 10 m and 30 m was studied to determine the presence of shallow cracks, which serve as channels for surface water to penetrate into the subsurface. On the other hand, isoresistivity at 80 m is significant because in many basements complicated terrains, groundwater (in the weathered zone) is regularly found at this depth, or occasionally much deeper.

At depths of 10 m, 30 m, and 80 m, the resistivity steadily increases towards the northwestern half of the research region. This suggests a reduced occurrence or lack of fractures in the northern area. Additionally, a considerable rise in resistivity is detected in the region with coordinates 9°39'18.4"N latitude and 6°31'23.0"E longitude. Concerning the isoresistivity at 80 m, the resistivity values demonstrate a rising tendency towards the extreme western region, demonstrating a noticeable variance compared to the isoresistivity at 10 m and 30 m depths.

Isopach Map (Depth to Basement Map)

The Isopach Map, also known as the Depth to Basement Map, provides insights into the variations in depth to the basement across different areas. The map reveals a range of depth to basement values, spanning from 2 m to 13.5 m. Regions with depth values between 2 m and 6 m indicate shallow depths to the basement, while areas ranging from 6 m to 10 m represent moderate depths. The highest depths to the basement, ranging from 10 m to 13.5 m, are observed in specific areas (as depicted in Fig. 10).

Table 2
Borehole yield parameters.

Coordinates	Elevation (m)	Borehole Yield (m ³ /day)
09°39'15.6"N 006°31'41.5"E	284	56.52
09°39'7.6"N 006°31'43.5"E	278	81.96
09°39'5.7"N 006°31'39.3"E	280	364.26
09°39'25.4"N 006°31'26.7"E	295	Indeterminable
09°39'18.4"N 006°31'23"E	303	Indeterminable

Weathered Layer Map

The subsurface's uppermost layer, known as the weathered layer, consists of unconsolidated materials such as gravel, sand, and soil. This layer exhibits a mixed composition and is characterized by low velocity. The boundary separating the consolidated and weathered layers is referred to as the base of the weathered layer. The weathered thickness map displays contours representing the varying thicknesses of the weathered layer, while the weathered layer resistivity map shows the resistivity values specific to the weathered layer. These maps are depicted in Figs. 11 and 12, respectively. Fig. 12 illustrates the locations and their corresponding weathered layer thicknesses. Lower resistivity values in certain areas indicate the presence of moisture, which can manifest as water or other highly conductive materials.

Groundwater Potential Map

The groundwater potential map was developed by analyzing a wide range of datasets linked to various hydrogeological aspects. These datasets included information from yield tests, resistivity measurements of weathered layers, maps depicting the thickness of weathered layers, borehole yield test results, hydraulic conductivity measurements, and infiltration rates. To organize this diverse collection of data effectively, a systematic classification process was employed. This ensured that each dataset was carefully categorized based on its characteristics and significance. Subsequently, these categorized datasets were integrated using an overlay method within the ArcGIS software.

As a result of this synthesis, the groundwater potential map delineated three distinct zones: poor, moderate, and high groundwater potential regions. The regions labeled as high and moderate potential indicated areas with considerable groundwater availability. On the other hand, the poor potential zones highlighted regions where challenges may be encountered in extracting groundwater. It is important to note that the high groundwater potential zone covered a relatively smaller area compared to the moderate and low potential zones. The majority of the research area fell within the moderate potential zone, which was distributed across the study region. Following this, the poor potential zone was identified in specific areas. This groundwater potential map serves as a valuable resource for comprehending how groundwater potential is distributed across space. It offers insights

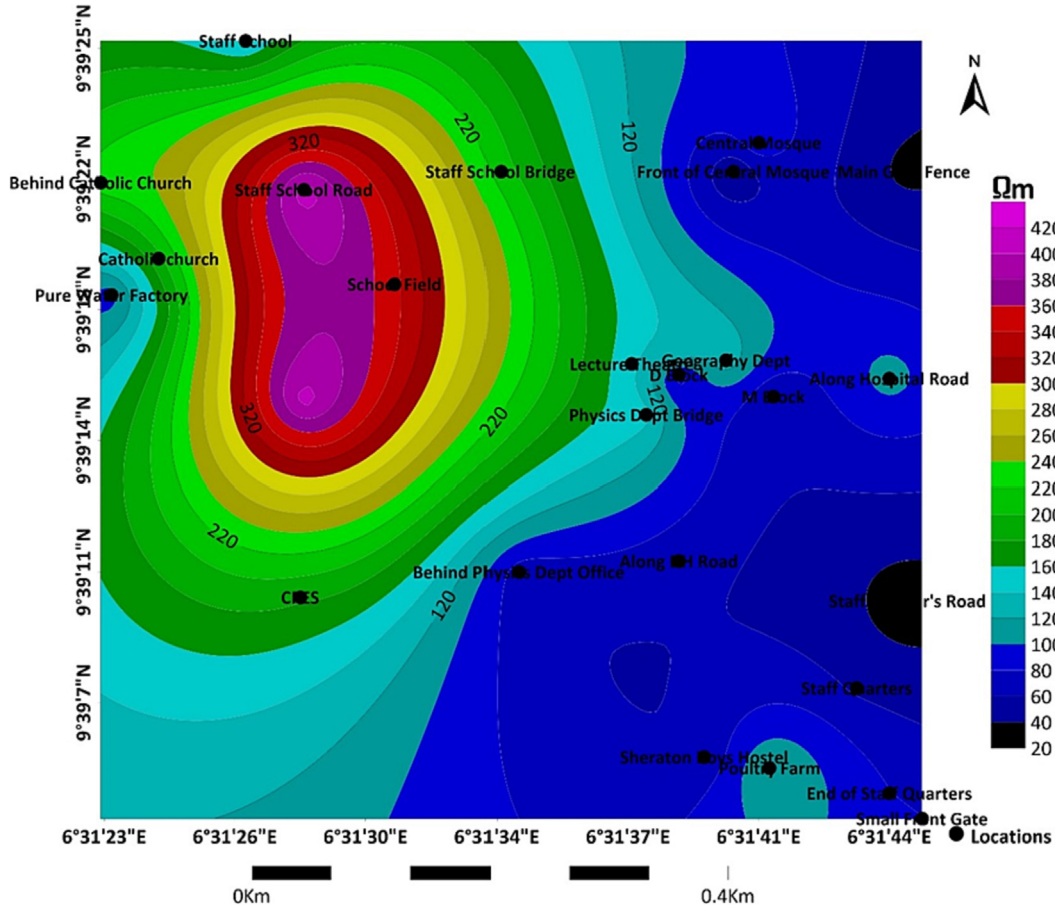


Fig. 7. Iso-resistivity map at 10 m.

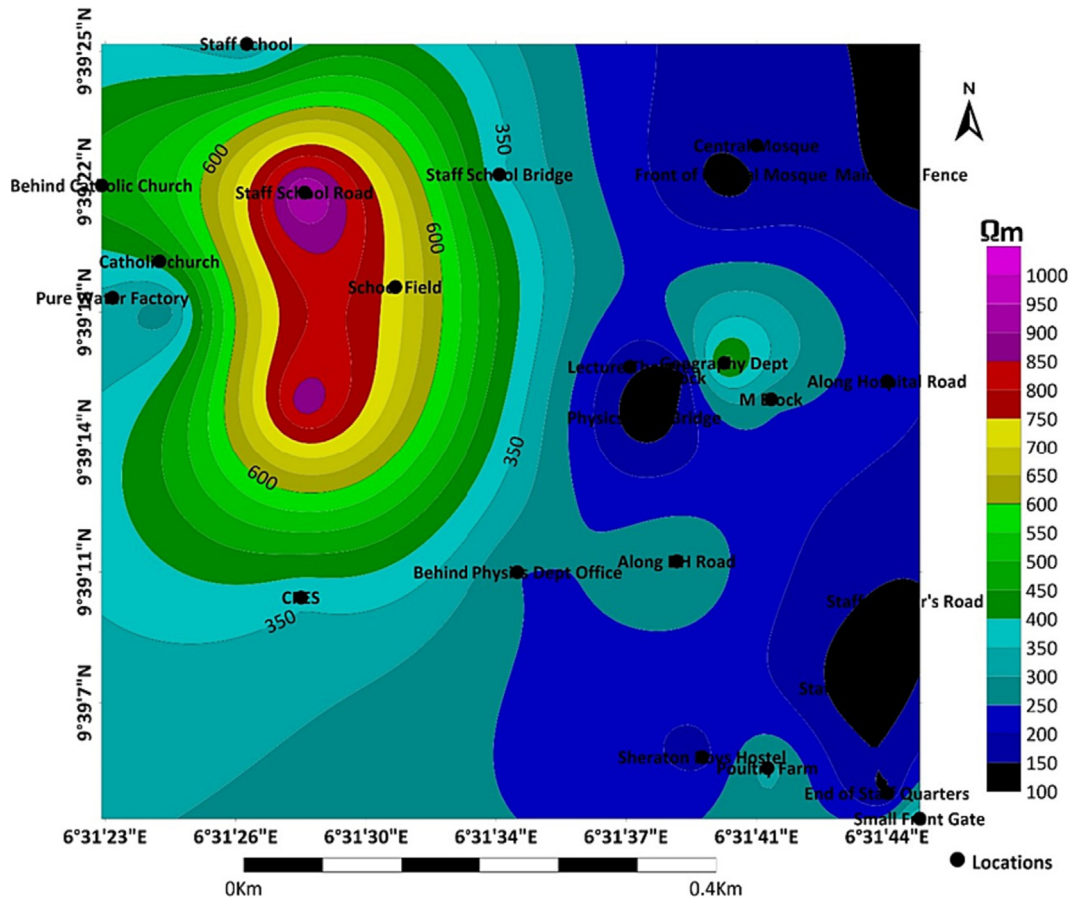


Fig. 8. Iso-resistivity map at 30 m.

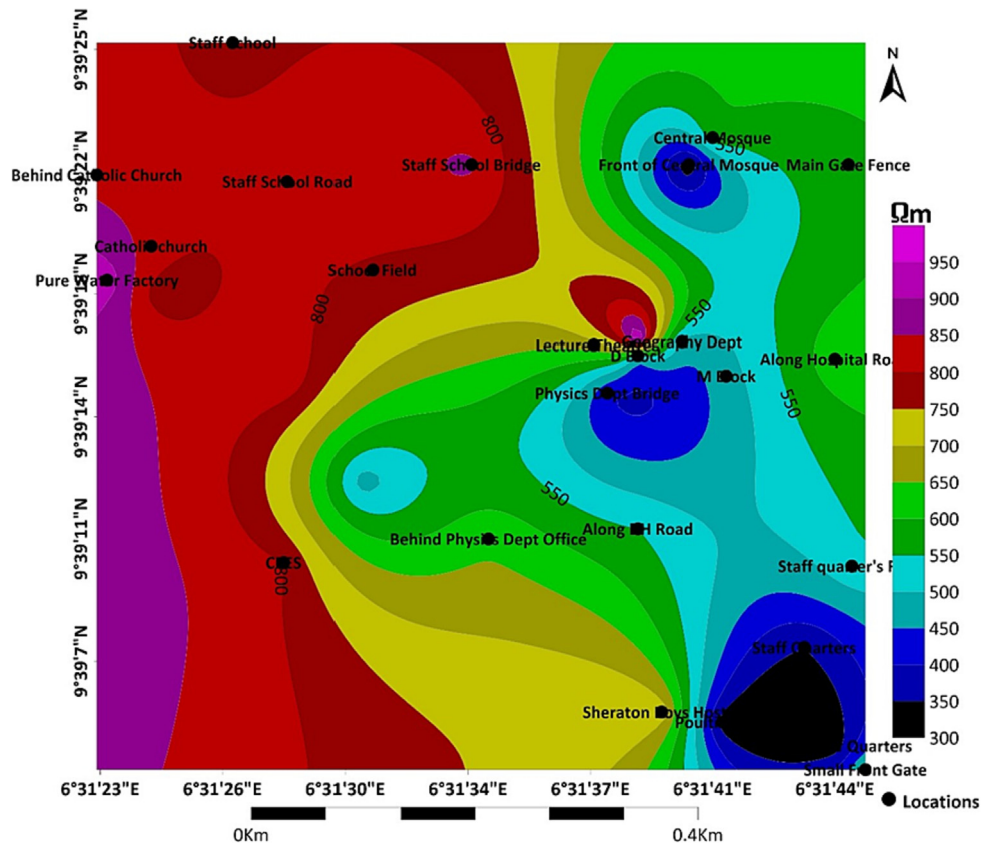


Fig. 9. Iso-resistivity map at 80 m.

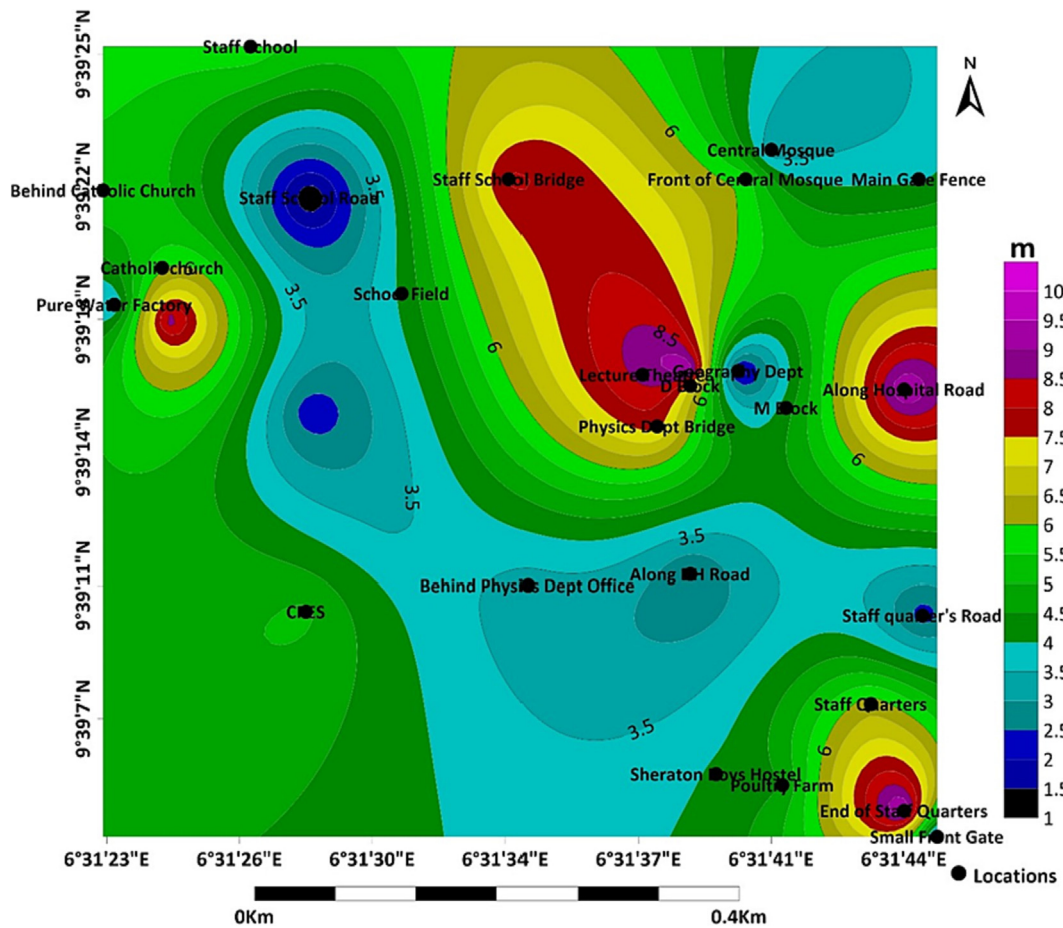


Fig. 10. Depth to Basement Map.

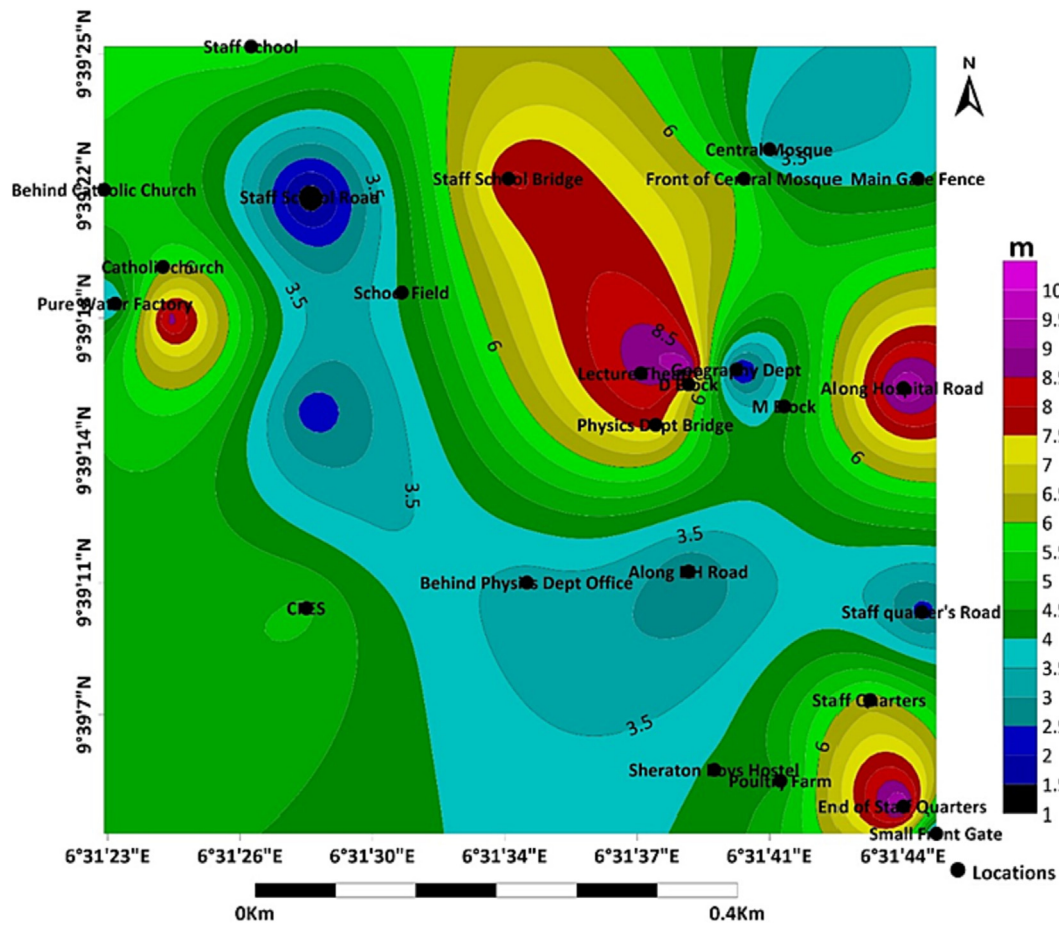


Fig. 11. Thickness of weathered layer map.

into the interplay of various hydrogeological factors and their combined influence on groundwater availability.

The groundwater potential map identified sites with varying levels of groundwater potential. Near the staff school, pure water factory, central mosque side, main school gate fence side, school field, physics department office, D-block, and poultry farm side, we observed low groundwater potential. On the other hand, sites such as the Catholic church, staff school road, staff bridge side, physics department bridge, hospital road, tiny main gate (staff quarters side), and staff quarters displayed moderate groundwater potential. Notably, the education-technology block, Sheraton boys' hostel, staff quarter road, DH Road, M Block, Geography Department, lecture theater, and Catholic church emerged as high-potential sites. The remaining areas were categorized as having moderate groundwater potential (Fig. 13).

Discussion

Characterizing subsurface geologic and hydraulic heterogeneities within crystalline basement aquifers presents considerable challenges (Offerdinger et al., 2019). Conventional methods involving drilling, core sample retrieval, and test well installation within crystalline basement rocks are not only arduous and costly but also limited in capturing spatial variations in hydrogeological properties (Doro et al., 2020). Even low-cost 1D geophysical techniques, such as Vertical Electrical Sounding (VES) commonly used in Nigeria, have demonstrated limitations (Alle et al., 2018).

In this study, an integrated approach was employed, combining geological, hydrogeological, and electrical measurements, alongside pumping test data, to comprehensively characterize the aquifer architecture of the area. Locations displaying higher moisture content

percentages typically indicate enhanced water-retention potential, which can be indicative of reduced permeability. Conversely, areas with lower moisture content percentages may suggest increased permeability and porosity, facilitating efficient water movement. These observations align harmoniously with the findings from the soil moisture content analysis, which consistently reveal the permeable and porous nature of the soil. This characteristic is underscored by the prevalence of coarse to fine sand grains, signifying favorable conditions for subsurface water movement.

Furthermore, the computed hydraulic conductivity values ranged from 7.00×10^{-5} m/s to 4.31×10^{-4} m/s, falling within the acceptable range for fine to coarse grain sands. Notably, the weathered zone typically exhibited lower hydraulic conductivity compared to the fractured zone with secondary connectivity. Variations in hydraulic conductivity across the study area serve to emphasize the inherent heterogeneity in permeability. The hydraulic conductivity map effectively delineates regions characterized by differing water flow potential, highlighting the significant influence of geological and hydrogeological attributes. Specifically, the south-eastern regions, where higher permeability is observed, correspond to areas with more favorable conditions for water movement. This reinforces the pivotal role played by geological features in governing groundwater dynamics within the study area.

The interpretation of the VES results provided valuable insights into aquifer attributes. The top layer, referred to as the regolith, exhibited apparent resistivity values ranging from 14 Ωm to 572 Ωm, with a thickness spanning from 0.5 m to 4.6 m. This layer primarily consists of silty and sandy clays, indicating chemical weathering of the crystalline rocks. Notably, the regolith layer is characterized by a substantial clay content and a thickness exceeding 3 m. While this can enhance the protective capacity of the underlying aquifer (Adabanija and Ajibade,

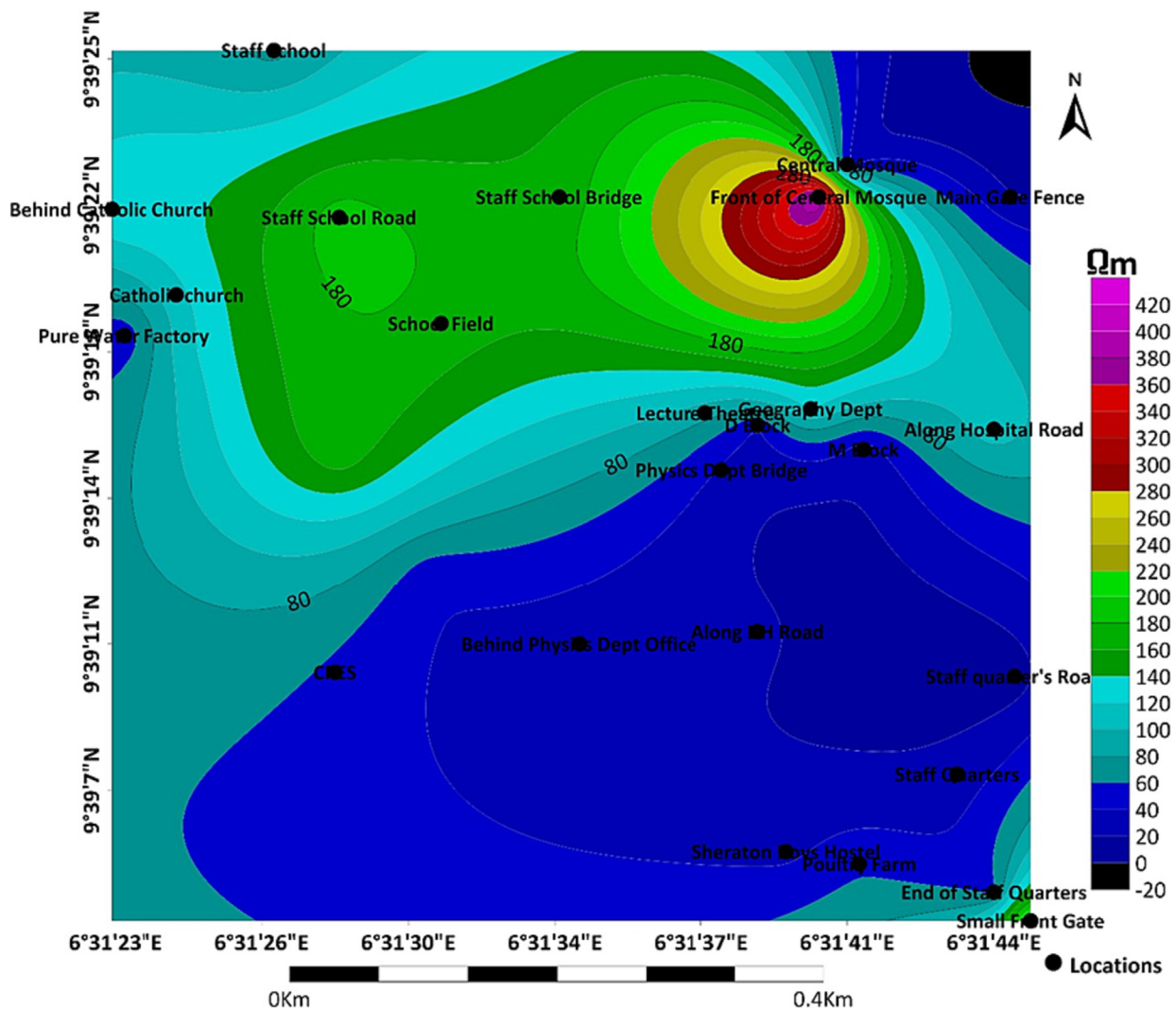


Fig. 12. Weathered layer resistivity map.

2020), it may significantly impede infiltration capacity and aquifer recharge (Akurugu et al., 2020).

The subsequent layer, known as the weathered layer or saprolite, displayed apparent resistivity values ranging from 10 Ωm to 407 Ωm , with a thickness ranging from 2.0 m to 13.1 m. This layer exhibited decreased resistivity in the resistivity model. Locations with relatively higher resistivity are indicative of less weathering activity and typically correspond to aquiferous units, given their tendency to remain saturated. However, it's essential to note that groundwater yield is influenced by factors such as formation grain connectivity, clay thickness, and regolith thickness (Taylor, 2001). The third layer, representing the bedrock, displayed apparent resistivity values ranging from 1468 Ωm to 1903 Ωm , with an infinite thickness. This layer is typically unfractured, except in specific cases where regional tectonics come into play. Consequently, the VES results facilitated the estimation of weathered and fractured zone thicknesses, crucial for predicting potential locations for water wells.

Conclusion

A mix of geological, hydrogeological, and geophysical techniques were used to estimate groundwater potential on the Bosso Campus of the Federal University of Technology, Minna. Field investigation confirmed the existence of fractured granitic rocks and a thin

regolith layer, indicating excellent places for boreholes. These broken rocks acted as channels for groundwater penetration and movement.

To examine groundwater potential, data on soil moisture content and infiltration rates were also used. Moisture percentage variations across places revealed changes in permeability, with some areas having impermeable layers and others having greater permeability. Surface water moved quicker into groundwater in the southern section of the research area than in the northwestern part.

The findings of high groundwater potential zones were validated by yield test data from selected boreholes, giving further evidence to verify existing hydrogeological maps and results. All available data, including sieve analysis for hydraulic conductivity, soil moisture content, infiltration rate experiments, depth to basement, weathered layer resistivity, thickness of the weathered layer, groundwater potential, and isoresistivities, were integrated to create a comprehensive groundwater potential map. Based on the combined parameters, the generated map classified different places as having low, moderate, or high groundwater potential.

Authors Contribution

JMO: Conceptualization of the study, Supervision and guidance throughout the research project, Analysis and interpretation of the

- Alle, I.C., Descloîtres, M., Vouillamoz, J.-M., Yalo, N., Lawson, F.M., Adihou, A.C., 2018. Why 1D electrical resistivity techniques can result in inaccurate siting of boreholes in hard rock aquifers and why electrical resistivity tomography must be preferred: the example of Benin, West Africa. *J. Afr. Earth Sci.* 139, 341–353. <https://doi.org/10.1016/j.jafrearsci.2017.12.007>.
- Amadi, A.N., Ameh, I.M., Idris-Nda, A., Okoye, N.O., Ejirofor, C.I., 2013. Geological and geophysical investigation of groundwater in part of Paiko, sheet 185, North Central Nigeria. *Int. J. Eng. Res. Dev.* 6 (1), 1–8.
- Anomohanran, O., 2013. Evaluation of aquifer characteristics in Echi, Delta State, Nigeria using well logging and pumping test method. *Am. J. Appl. Sci.* 10 (10), 1263–1269. <https://doi.org/10.3844/ajassp.2013.1263.1269>.
- Anomohanran, O., 2015. Hydrogeophysical investigation of aquifer properties and lithological strata in Abraka, Nigeria. *J. Afr. Earth Sci.* 102, 247–253. <https://doi.org/10.1016/j.jafrearsci.2014.10.006>.
- Anomohanran, O., Iserhien-Emekeme, R.E., 2014. Estimation of aquifer parameters in Erho, Nigeria using the cooper-jacob evaluation method. *Am. J. Environ. Sci.* 10 (5), 500–508. <https://doi.org/10.3844/ajessp.2014.500.508>.
- Ayolabi, E., Adedeji, J., Oladapo, I., 2004. A geoelectric mapping of Ijapo, Akure Southwest Nigeria and its hydrogeological implications. *Global J. Pure Appl. Sci.* 10 (3). <https://doi.org/10.4314/gjpas.v10i3.16420>.
- Balasubramanian, A., 2017. Procedure for conducting pumping tests. *Indian Soc. Sci. Congr.-Trends Earth Sci. Res.* <https://doi.org/10.13140/RG.2.2.18948.32641.1>.
- Domenico, P.A., Schwartz, F.W., 1998. *Physical and Chemical Hydrogeology*. Wiley.
- Doro, K.O., Adegboyega, C.O., Aizebeokhai, A.P., Oladunjoye, M.A., 2020. Hydrological variability in crystalline basement aquifers—insight from a first hydrogeophysics research site in Nigeria. *Proceedings of the NSG2020 26th European Meeting of Environmental and Engineering Geophysics, Amsterdam, Netherlands, 7–8 December 2020*. Vol. 2020, pp. 1–5.
- Ejepu, J.S., 2020. Regional assessment of groundwater potential zone using remote sensing, GIS and Multi Criteria Decision Analysis Techniques. *Niger. Ann. Pure Appl. Sci.* 3 (3b), 99–111. <https://doi.org/10.46912/napas.201>.
- Ejepu, S., Olasehinde, P., 2014. Groundwater potential evaluation of a part of Gidan Kwano campus of the Federal University of Technology, Minna, Central Nigeria using GEOELECTRIC methods. *Niger. J. Tech. Res.* 9 (1), 43. <https://doi.org/10.4314/njtr.v9i1.7>.
- Ejepu, J.S., Olasehinde, P., Okhimamhe, A., Okunlola, I., 2017. Investigation of hydrogeological structures of Paiko region, north-central Nigeria using integrated geophysical and remote sensing techniques. *Geosciences* 7 (4), 122. <https://doi.org/10.3390/geosciences7040122>.
- Ejepu, J.S., Jimoh, M.O., Abdullahi, S., Mba, M.A., 2022. Groundwater exploration using multi criteria decision analysis and analytic hierarchy process in Federal Capital Territory, Abuja, Central Nigeria. *Int. J. Geosci.* 13 (01), 33–53. <https://doi.org/10.4236/ijg.2022.131003>.
- Epuh, E.E., Orji, M.J., Iyoyojie, H.A., Daramola, O.E., 2020. Groundwater potential mapping in Ikorodu, Lagos State, Nigeria, using multi-criteria analysis and hydrogeophysics. *Niger. J. Technol.* 39 (1), 278–292. <https://doi.org/10.4314/njt.v39i1.31>.
- Federal Meteorological Agency, 2011. *Minna Weather Report Unpublished*.
- George, N.J., Agbasi, O.E., Umoh, J.A., Ekanem, A.M., Ejepu, J.S., Thomas, J.E., Udoinyang, I.E., 2022. Contribution of electrical prospecting and spatiotemporal variations to groundwater potential in coastal hydro-sand beds: a case study of Akwa Ibom State, Southern Nigeria. *Acta Geophys.* 71 (5), 2339–2357. <https://doi.org/10.1007/s11600-022-00994-2>.
- Gomo, M., 2018. On the interpretation of multi-well aquifer-pumping tests in confined porous aquifers using the cooper and jacob (1946) method. *Sustain. Water Resour. Manag.* 5 (2), 935–946. <https://doi.org/10.1007/s40899-018-0259-z>.
- Ian, P., & Charles, G. (2019). *Determination of Moisture Content in Soil*. JoVE, Cambridge, MA. Arizona University JoVE Science Education Database. Environmental Microbiology. Retrieved from <https://www.jove.com/science-education/10011/determination-of-moisture-content-in-soil>. 02/04/2020.
- Ifeanyichukwu, K.A., Okeyeh, E., Agbasi, O.E., Moses, O.I., Ben-Owope, O., 2021. Using geoelectric techniques for vulnerability and groundwater potential analysis of aquifers in Nnewi, South Eastern Nigeria. *J. Geol. Geogr. Geocol.* 30 (1), 43–52. <https://doi.org/10.15421/112105>.
- Newman, C.P., Kisfalusi, Z.D., Holmberg, M.J., 2021. Assessing specific-capacity data and short-term aquifer testing to estimate hydraulic properties in alluvial aquifers of the Rocky Mountains, Colorado, USA. *J. Hydrol. Reg. Stud.* 38, 100949. <https://doi.org/10.1016/j.ejrh.2021.100949>.
- Nigerian Meteorological Agency, (2019). *Seasonal Rainfall Prediction (SRP)*, Retrieved from <https://fscluster.org/nigeria/document/nigerian-meteorological-agency-nimet.06/01/2020>
- Offodile, M.E., 2002. *Groundwater Study and Development in Nigeria*. Mecon Geology and Engineering Services Ltd., Jos, Nigeria.
- Offerdinger, U., MacDonald, A.M., Comte, J.-C., Young, M.E., 2019. Groundwater in fractured bedrock environments: managing catchment and subsurface resources – an introduction. *Geol. Soc. Lond. Spec. Publ.* 479 (1), 1–9. <https://doi.org/10.1144/sp479-2018-170>.
- Olarewaju, V.O., Olorunfemi, M.O., & Alade, O., 1996. Chemical characteristics of groundwater from some parts of the Basement Complex of central Nigeria. *J. Mining Geol.* 33 (2), 135–139.
- Olasehinde, P.I., 1999. An integrated geologic and geophysical exploration technique for groundwater in the basement complex of west-central part of Nigeria. *Water Resour. J. Niger. Assoc. Hydrogeol.* 10 (1), 46–49.
- Olorunfemi, M.O., Fasuyi, S.A., 1993. Aquifer types and the geoelectric/hydrogeologic characteristics of part of the Central Basement Terrain of Nigeria (Niger state). *J. Afr. Earth Sci.* 16 (3), 309–317. [https://doi.org/10.1016/0899-5362\(93\)90051-q](https://doi.org/10.1016/0899-5362(93)90051-q).
- Oyedele, A.A., 2019. Use of remote sensing and GIS techniques for groundwater exploration in the basement complex terrain of ado-Ekiti, SW Nigeria. *Appl Water Sci* 9 (3). <https://doi.org/10.1007/s13201-019-0917-9>.
- Reinhard, K., 2006. *Groundwater Geophysics, A tool of Hydrogeology: Geoelectrical Method*. Springer Berlin Heidelberg New York, Hamburger, Germany, pp. 85–87.
- Robinson, D.A., Campbell, C.S., Hopmans, J.W., Hornbuckle, B.K., Jones, S.B., Knight, R., Ogden, F., Selker, J., Wendroth, O., 2008. Soil moisture measurement for ecological and hydrological watershed-scale observatories: a review. *Vadose Zone J.* 7 (1), 358–389. <https://doi.org/10.2136/vzj2007.0143>.
- Sikakwe, G.U., 2018. GIS-based model of groundwater occurrence using geological and hydrogeological data in Precambrian Oban Massif Southeastern Nigeria. *Appl Water Sci* 8 (3). <https://doi.org/10.1007/s13201-018-0700-3>.
- Singh, S.K., 2001. Confined aquifer parameters from temporal derivative of drawdowns. *J. Hydraul. Eng.* 127 (6), 466–470. [https://doi.org/10.1061/\(asce\)0733-9429\(2001\)127:6\(466\)](https://doi.org/10.1061/(asce)0733-9429(2001)127:6(466)).
- Sophocleous, M., 2000. From safe yield to sustainable development of water resources—the Kansas experience. *J. Hydrol.* 235 (1–2), 27–43. [https://doi.org/10.1016/S0022-1694\(00\)00263-8](https://doi.org/10.1016/S0022-1694(00)00263-8).
- Taylor, R., 2001. Weathered rock aquifers: vital but poorly developed. *Waterlines* 20 (2), 3–6. <https://doi.org/10.3362/0262-8104.2001.047>.
- Trabelsi, R., Zouari, K., Kammoun, S., Trigui, M.R., 2020. Recharge and Paleo-recharge of groundwater in different basins in Tunisia. *Quat. Int.* 547, 152–165. <https://doi.org/10.1016/j.quaint.2019.04.026>.